GDCh Research Article Angewandte International Edition Chemie www.angewandte.org

How to cite: *Angew. Chem. Int. Ed.* **2025**, *64*, e202413383
doi.org/10.1002/anie.202413383

Electrochemistry

Electrochemical C–O and C–N Arylation using Alternating Polarity in flow for Compound Libraries

Jennifer Morvan, Koen P. L. Kuijpers, Dayne Fanfair, Bingqing Tang, Karolina Bartkowiak, Lars van Eynde, Evelien Renders, Jesus Alcazar, Peter J. J. A. Buijnsters, Mary-Ambre Carvalho, and Alexander X. Jones**

Abstract: Etherification and amination of aryl halide scaffolds are commonly used reactions in parallel medicinal chemistry to rapidly scan structure–activity relationships with abundant building blocks. Electrochemical methods for aryl etherification and amination demonstrate broad functional group tolerance and extended nucleophile scope compared to traditional methods. Nevertheless, there is a need for robust and scale-transferable workflows for electrochemical compound library synthesis. Herein we describe a platform for automated electrochemical synthesis of C–X arylation (X=NH, OH) in flow to access compound libraries. A comprehensive Design of Experiment (DoE) study identifies an optimal protocol which generates high yields across > 30 aryl halide scaffolds, diverse amines (including electron-deficient sulfonamides, sulfoximines, amides, and anilines) and alcohols (including serine residues within peptides). Reaction sequences are automated on commercially available equipment to generate libraries of anilines and aryl ethers. The unprecedented application of potentiostatic alternating polarity in flow is essential to avoid accumulating electrode passivation. Moreover, it enables reactions to be performed in air, without supporting electrolyte and with high reproducibility over consecutive runs. Our method represents a powerful means to rapidly generate nucleophile independent C–X arylation compound libraries using flow electrochemistry.

Introduction

Aryl-Alkyl ethers and anilines are recurring motifs in medicinal chemistry. High-throughput synthesis and testing of aryl C–O and C–N compound libraries accelerates structure-activity relationship exploration. Alkyl alcohols and amines are among the most abundant and diverse building blocks for library synthesis,[1] enabling exploration of a broad chemical space to improve overall biological profile and accelerate lead compound identification.

Library synthesis is facilitated by generally applicable reaction conditions, tolerant of diverse coupling partners and functional groups.[2] Buchwald–Hartwig Pd-[3] and Ullmann type Cu-catalyzed methods[4] for amination of an aryl halide scaffold are well established. C–O coupling can be achieved by similar methods although is typically more challenging due to the lower nucleophilicity of alcohols.[5] Reaction success is strongly ligand-dependent across scaffold and nucleophile class. Recently, nickel-catalyzed electrochemical[6] and photoredox[7] C–O and C–N couplings have been added to the toolbox.[8] We were impressed by the extended nucleophile scope of these emerging methods, applicable across nucleophile classes (X=NH, OH, SH, CO_2H), sometimes without ligand variation,[7a] which would enable incorporation of more diverse nucleophiles into C–X arylation libraries. Significant efforts have been placed into expanding the use of photoredox reactions in library synthesis by incorporating lab automation[1a,9] and critical comparisons of available equipment to ensure reproducibility.[10] These efforts have greatly increased adoption in industry.

Electrochemistry has the additional benefit of being able to control cell current and voltage as continuous parameters to achieve high levels of chemo-,[11] regio-selectivity[12] and functional group tolerance.[13] Despite this promise, industry adoption is slow due to a lack of standardized equipment and workflows for electrochemical library synthesis.[14] Several reactors are commercially available for batch parallel[14b,15] and flow synthesis.[16] However, poor reproducibility is observed when transferring between reactors or

[*] J. Morvan, B. Tang, K. Bartkowiak, L. van Eynde, E. Renders, P. J. J. A. Buijnsters, M.-A. Carvalho, A. X. Jones
Global Discovery Chemistry, Janssen Research and Development, Turnhoutseweg 30, 2340 Beerse, Belgium
E-mail: ajones40@its.jnj.com
mcarva11@its.jnj.com
K. P. L. Kuijpers, D. Fanfair
API SM Technology, Janssen Research and Development, Turnhoutseweg 30, 2340 Beerse, Belgium
J. Alcazar
Chemical Capabilities, Analytical & Purification, Global Discovery Chemistry, Janssen-Cilag, S.A., C/Jarama 75, 45007 Toledo, Spain

reaction scales (e.g. High Throughput Experiment (HTE) to preparative scales), and inconsistent results are often observed across batch parallel reactors, due to lack of electrochemical control of individual wells.[15,17] Single-pass flow electrochemistry offers several advantages over batch, including smaller interelectrode distances and greater electrode area-to-cell volume ratios,[16,17,18] which enhance mass transfer and accelerate reaction times. The challenge here is to balance high conversion with reactor productivity (mmol/h of product) in continuous flow and to avoid electrode passivation through time which can deteriorate conversion or selectivity (Figure 1B).

Electrochemical C–X arylation was first reported by Li et al.[6a] Further publications from Baran,[6b,c] Rueping[6e] and Semenov[6d] demonstrated that reaction conditions in batch could be adapted across nucleophile classes (X=NH, OH, CO_2H) by varying the basic additive and application of alternating current (AC) (Figure 1A). However, implementation for parallel synthesis has been lacking, although highly desired.

Recently, Rial-Rodriguez et al. published an innovative platform for electrochemical C–N arylation of brominated Cereblon ligands in flow. Single-pass slug flow enabled automated reaction sequences on HTE-scale ($\leq$10 µmol).[18]

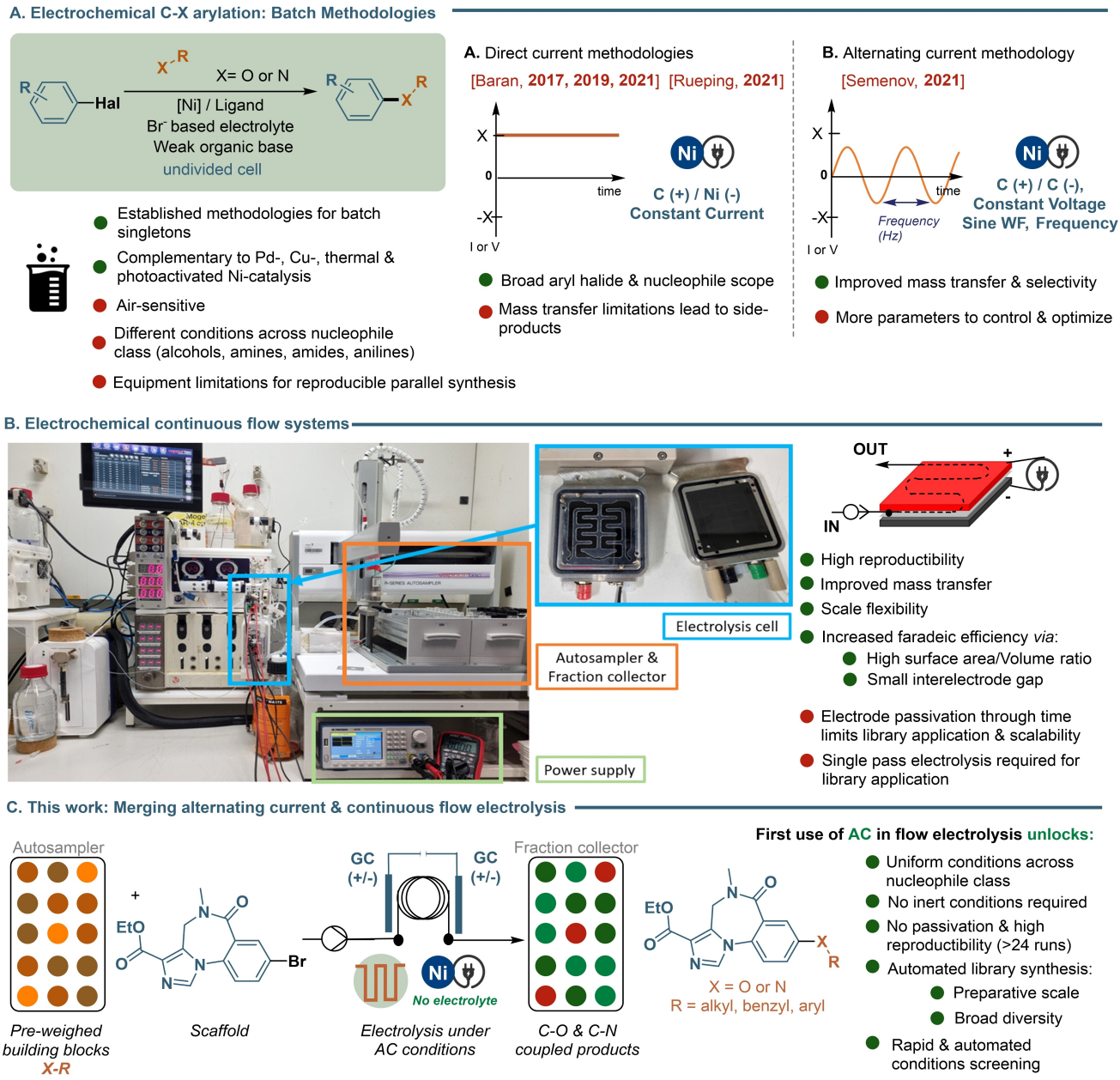

Figure 1. State of the art in singleton electrochemical C–X arylation (A); electrochemical continuous flow systems (B) and our strategy for continuous flow electrocatalyzed C–X arylation automated compound library synthesis (C). WF=Wave Form. Hal = Halogen

Herein, we describe an extended platform for automated electrochemical synthesis of C–X arylation (X=NH, OH) libraries in flow (figure 1B & C). Our methodology is designed for general applicability across diverse aryl halides and nucleophiles, rather than single reaction optimization. Consistent performance over sequential runs and across reaction scales (25 µmol–10 mmol) is unlocked by the unprecedented application of alternating polarity in flow.[19] This is essential to avoid accumulating electrode passivation,[19e] and enables reactions to be performed in air, without supporting electrolyte (Figure 1C). This breakthrough also allows fast conditions screening in sequential runs. A comprehensive DoE identified important non-linear interactions between chemical and electrochemical parameters as well as optimal reaction conditions resulting in the employment of a single set of electrochemical conditions for the automated synthesis of over 100 diverse C–O and C–N arylation products without the need for ligand or base variation. Of note for medicinal chemistry are the late-stage heterofunctionalization of drug derivative compounds, cereblon binders and amino acids. The nucleophile scope encompasses both e-rich and e-deficient amines (e.g. sulfonamides, sulfoximines, anilines), alcohols and serine-containing peptide.

Results and Discussion

Preliminary Study with DC Current

We initially investigated the C–O coupling reaction in parallel batch and flow devices. The model reaction between 4-trifluoromethyl-bromobenzene (**1**) and 3-hydroxytetrahydrofuran (**2**) was initially performed with the Analytical Sales 24-well HTe-chem device[14b] using conditions from Semenov[6d] (Conditions 1—although with direct current (DC) as AC input is not available with the device) and Baran[6c] (conditions 2). Reactions were run to both 4 and 6 *F*/mol total charge. Poor yields of product **3a** were obtained mainly because of the formation of debrominated **3c**, as well as inconsistent results across the plate (figure 2A). For example, at 1 mA (current density 2 mA.cm^{-2}), with conditions 2, **3a** yields ranged from 8–25 % at 4 *F*/mol and 2–35 % at 6 *F*/mol. We switched to the Vapourtec ION electrochemical flow[21] reactor with two glassy carbon (GC) electrodes at 30 mA constant current (2.5 mA/cm^2), 15 mol % $NiBr_2$.glyme catalyst, bipyridine ligand, quinuclidine base and lithium bromide electrolyte (conditions, figure 2B'). Yields of desired ether **3a**, aryl-aryl (Ar–Ar) coupling **3b** and trifluorobenzene (**3c**) were monitored by calibrated LCMS (Liquid Chromatography-Mass Spectroscopy). Three different electrode spacings were

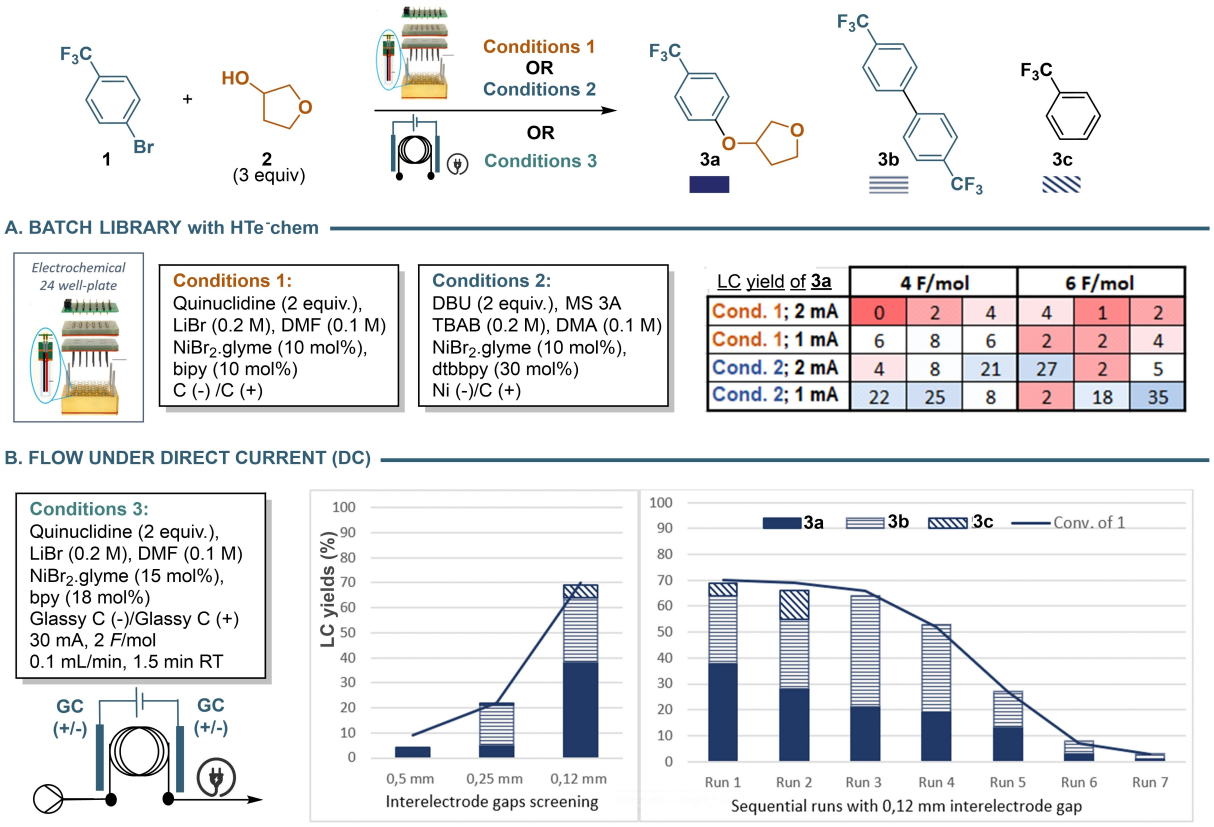

Figure 2. Preliminary tests of C–O arylation in library mode with (A) HTe-Chem parallel batch device and (B) Sequential flow ION reactor under direct current (DC). Graphs show influence of the interelectrode gaps of the model reaction and results over 7 sequential runs (100 µmol each) in DC mode. LC (Liquid Chromatography) yields were determined thank to calibration curve. RT = Residence time.

investigated 0.12 mm, 0.25 mm and 0.5 mm by varying the thickness of the interelectrode membrane. The aryl etherification reaction proceeds via a paired-electrolysis mechanism, requiring rate-limiting catalyst diffusion between electrodes for turnover (see references 6c and 6d for mechanistic discussion).[6c,d] Studies on related paired-electrolysis reactions have demonstrated that minimizing electrode spacing accelerates mass transfer.[22] Indeed, at the lower interelectrode gap (0.12 mm), we observed improved substrate conversion (70 %), product **3a** yield (38 %) and selectivity (18 % **3b**, 4 % **3c**). The residence time (RT) in the reactor was only 1.5 minutes corresponding to 2 *F*/mol total charge at 30 mA, indicating greater faradaic efficiency compared to the parallel batch device.

However, sequential reactions at 0.12 mm electrode distance showed substantial deterioration of product yield and reaction selectivity, even with intermediate solvent or air washing, due to the passivation of the GC anode (Figure 2). Similar deterioration was observed in a model C–N coupling reaction (see Supporting Information, Figure S2). Higher yields could only be regained after abrasive washing with Celite suspension. This highlights the challenges of transferring between HTE (<10 µmol) scales described by Rial-Rodriguez et al.[18] and preparative scales (≥ 100 µmol) as the effects of accumulating passivation take longer to be observed on smaller scales.

Reaction Optimization: One Parameter at a Time

We rationalized that application of an alternating current may help to reduce electrode fouling[19e,23] and simultaneously accelerate the reaction.[6d] Bortnikov et al. elegantly demonstrated that slow alternating polarity (0.5–25 Hz sine wave) accelerates nickel-catalyzed C–X arylation in a batch reactor. Since both oxidative and reductive redox steps occur successively at the same electrode, diffusion limitations are effectively eliminated.[6d] Indeed, we found that the application of a 1 Hz square waveform (SqWF) with 3.0 V (6.0 Volt $_{\text{peak-to-peak}}$ (Vpp)) to our model reaction gave a 32 % LC yield of **3a** reproducibly over 24 reactions and improved selectivity (1 % Ar–Ar coupling and 0 % dehalogenation), with a residence time of only 1.5 mins (data not shown). So far, this example is the first application of AC for continuous flow electrolysis.

The consistency of results enabled high-throughput screening in flow to optimize the model reaction and understand the influence of discrete and continuous parameters on yield and selectivity (Figure 3A). Automated injections and collections were performed using an autosampler. Reagents and catalyst solutions were injected in separate lines and pre-mixed through a mixing chip before entering the reactor, as prolonged standing (24 h) of the nickel catalyst with substrates led to reduced yields.

Nickel catalyst and ligand screening (Figure 3A and Supporting Information Figure S6, S7) indicated a preference for 4–4 -dimethoxy-2–2 -bipyridine (OMe_2bipy) and $NiCl_2$.glyme, improving product formation up to 40 % LC yield with less than 1 % formation of aryl-aryl coupling **3b** and dehalogenation **3c**. The base strongly influenced conversion and selectivity: replacing quinuclidine with 1,4-diazabicyclo [2.2.2]octane (DABCO), 1,8-diazabicyclo-[5.4.0]undec-7-ene (DBU), or *N*-methylpiperidine led to reduced yield and mass balance (Figure 3 and Supporting Information Figure S8). Acyclic tertiary amines such as triethylamine (TEA) resulted in a drop in selectivity, consistent with the literature.[6d] Alternative electrode pairs were also investigated: Pt | Pt reduced selectivity, whereas graphite | graphite and Ni | Ni inhibited the reaction entirely. We were pleased to find that reactions could be set up and performed in air without loss in yield or selectivity. The lithium bromide supporting electrolyte was detrimental for sequential runs under AC conditions, reducing reaction yield from 40 % to 33 % after six reactions. The square waveform was also very important for decent yield since a drop from 40 to 13 % was observed when the sine waveform was applied due to lower RMS (Root-Mean-Square) cell voltage (15 mA, 1.5 mA.cm^{-2})

We envisioned performing a DoE optimization to investigate the influence of continuous reaction parameters such as AC frequency, voltage, substrate, base and nucleophile concentrations, temperature, and flow rate. Initial experiments were performed to define the boundaries of the exploration. Increasing voltage to 4 V (8 V_{pp}) improved yield to 52 % without loss of selectivity, whereas 2 V (4 V_{pp}) was insufficient for conversion. Altering the AC frequency to 0.1 Hz resulted in increased aryl-aryl coupling, tending towards the poor selectivity observed with DC (figure 2). Higher frequencies (≥ 3 Hz) reduced cell current (<20 mA, 2.0 mA.cm^{-2}) and conversion. Finally, applying a flow rate of 0.05 mL/min (3 min residence time), compared to 0.1 mL/min resulted in a 60 % LC yield of ether **3a**. A sequence of 24 runs under these conditions confirmed the reproducibility of the system, giving 81.8 % conversion ± 1.8 % and 61.1 % ± 0.9 % yield of **3a** across the sequence (Figure 3B).

DoE Optimization

Design of Experiments (DoE) provides a methodical approach to optimize product yield and identify statistically significant factors and factor interactions. A Box-Behnken design, which is a quadratic response surface design, was selected since it can identify all statistically significant primary factors, factor interactions and quadratic (non-linear) terms. The DoE consisted of 7 continuous factors: base equivalents, alcohol equivalents, substrate concentration, flow rate, AC frequency, peak to peak voltage and temperature. Three responses were modelled and optimized in the DoE: substrate conversion, yield of desired product **3a**, and selectivity (% yield of **3a**/%conversion of **1**). To achieve an optimal outcome, a total of 60 experiments were performed in the DoE, resulting in an improvement in isolated yield from 61 % to 74 %.

The DoE generation and subsequent data analysis were performed with JMP (DoE software). A stepwise regression was utilized to generate the response models, which were optimized by setting a desirability function for each

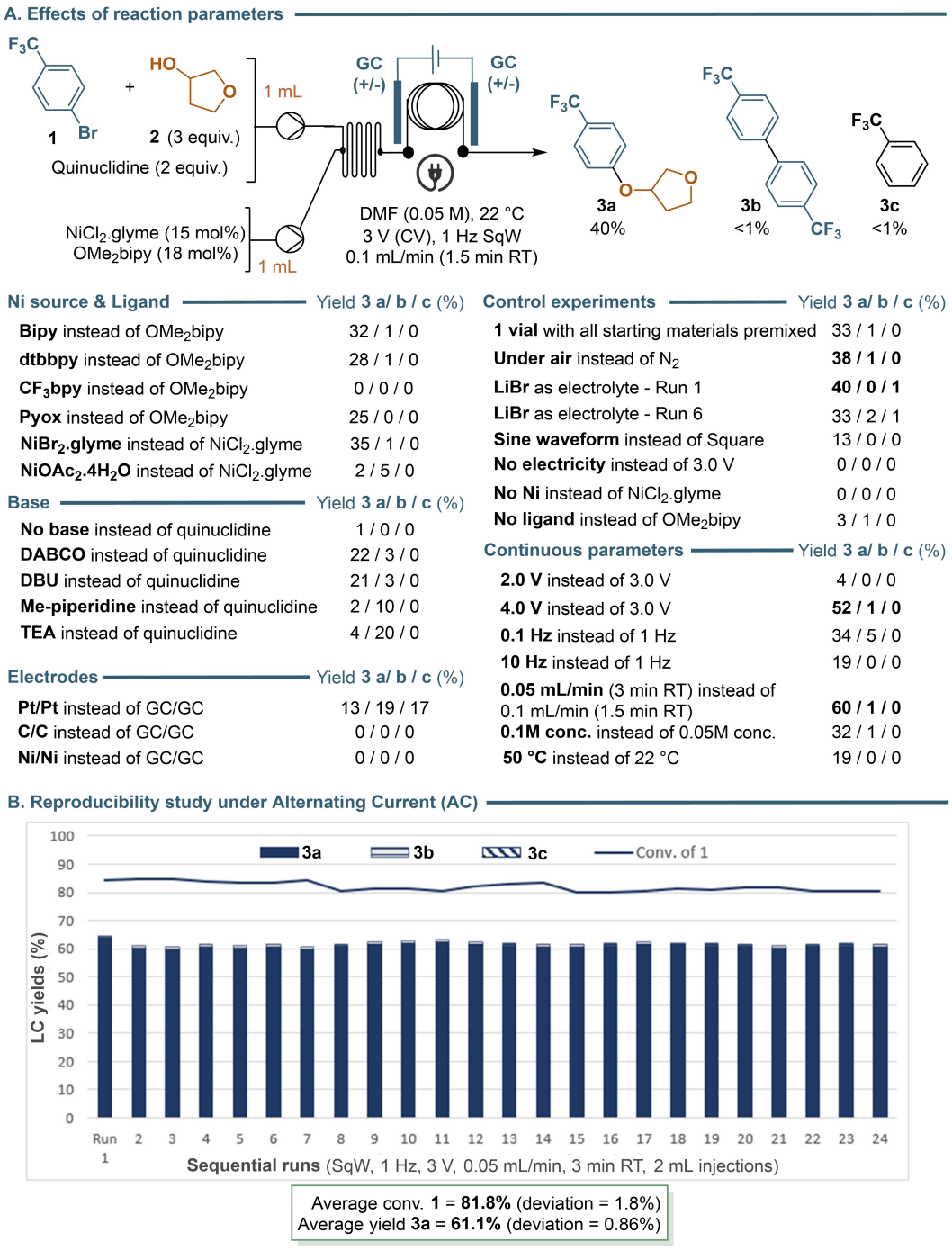

Figure 3. (A) Screening of discrete and continuous parameters and (B) results over 24 sequential runs (100 µmol each) in AC mode. LC yields of **3a**,**b**,**c** determined with calibration curves. (B) reproducibility study over 24 sequential runs (100 µmol scale).

response. An analysis was also performed to assess the relative importance of each factor, i.e., variable importance. A visual summary of this information is presented in Figure 4. The factors are ranked in order of decreasing variable importance, from left to right. The red-to-white gradient in the plots in Figure 4A corresponds to the total effect of the factors on each response, wherein red represents a relatively large total effect. The optimal values of each factor are shown in red at the bottom of Figure 4A.

An assessment of factor importance showed alcohol equivalents have the greatest total overall effect in the DoE and the greatest total effect (0.592) on selectivity. Voltage has the next greatest overall effect in the DoE and also a high total effect on substrate conversion (0.482) and yield (0.418). The optimal cell voltage (4 V) is in excess of the thermodynamic potential difference required from CV studies, 2.3 V, or the synthetically effective 3 V voltage applied by Bortnikov *et al.* in batch.[6d] However, in the

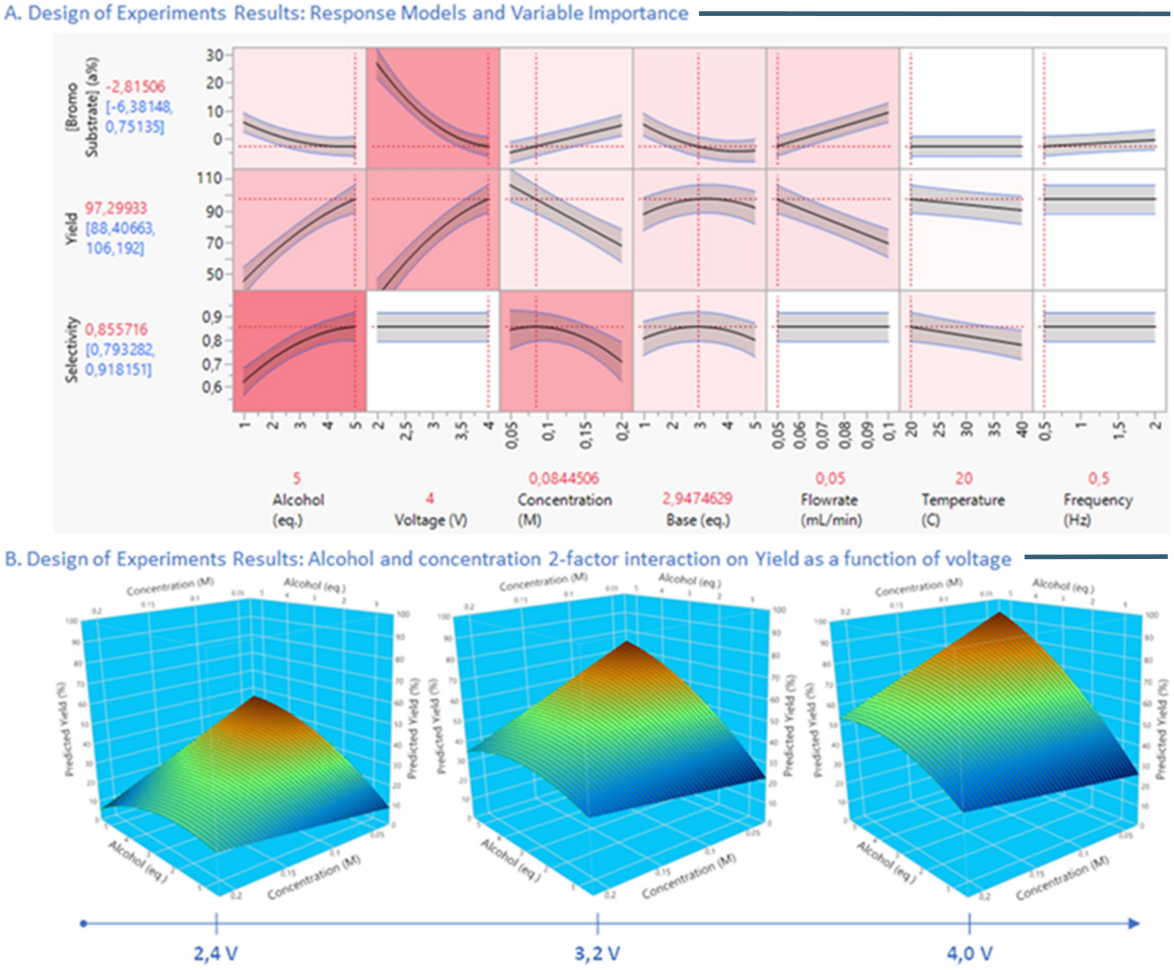

Figure 4. Summary of the Design of Experiment results with (A) each parameter model and (B) 2-factorial interactions between alcohols equivalent and concentration at different voltages.

absence of supporting electrolyte, only competing anodic *N,N*-Dimethyl-formamide (DMF) oxidation was a concern (+1.6 V vs. Saturated Calomel Electrode), which was allayed by the absence of electrode passivation.

Frequency has the weakest influence on substrate conversion, yield and selectivity within the parameter ranges investigated. A response model was also generated for **3b**, which varied between 0 and 2 %. This relatively low level of **3b**, under AC conditions, showed that the optimal frequency range was selected for the DoE.

The analysis of the DoE data revealed many statistically significant 2-factor interactions, an example of which is shown in Figure 4b. This is a powerful result as it shows a non-linear influence of alcohol, concentration, and voltage on yield. If for example, the alcohol equivalents were initially optimized with a high concentration (0.2 M), the yield would reach a maximum of 50–52 % at the highest voltage, whereas the global maximum requires simultaneous optimization of alcohol equivalents, concentration, and voltage. The main advantage of the DoE, in comparison to the traditional one factor at a time approach, is that much greater insight (faster) is gained from such 2-factor interactions which showed a pathway towards yields > 80 %.

JMP proposed the following optimal conditions based on the response models and the desirability functions: 2.9 equivalents of base, 5 equivalents of alcohol, a concentration of 0.08 M, a flowrate of 0.05 mL/min, a frequency of 0.5 Hz, 4 V, and 20 °C. Applying these conditions resulted in 96 % conversion, a selectivity of 77 % and a 74 % LC yield. These conditions were used to investigate the substrate scope, except for alcohol equivalents, which were lowered to 4 equivalents for reasons of reagent economy.

Substrate Scope

The optimal conditions for C–O coupling obtained from HTE and DoE were applied across a broad range of aryl halides using 3-hydroxy-THF (**2**) or *N*-Boc piperidine-4-propanol as nucleophiles (Figure 5). The model product **3a** could be obtained from aryl chloride, bromide or iodide precursors in 43 %, 66 % and 71 % isolated yields, respectively. Bromobenzenes with a range of functional groups, including ketones (**4**), esters (**5**,**6**,**9**,**10**), boronic ester (**7**), halogens (**8**–**10**, **13**, **18**), amides (**11**–**14**), sulfones (**15**–**16**), were tolerated due to the mild reaction conditions, i.e. mild

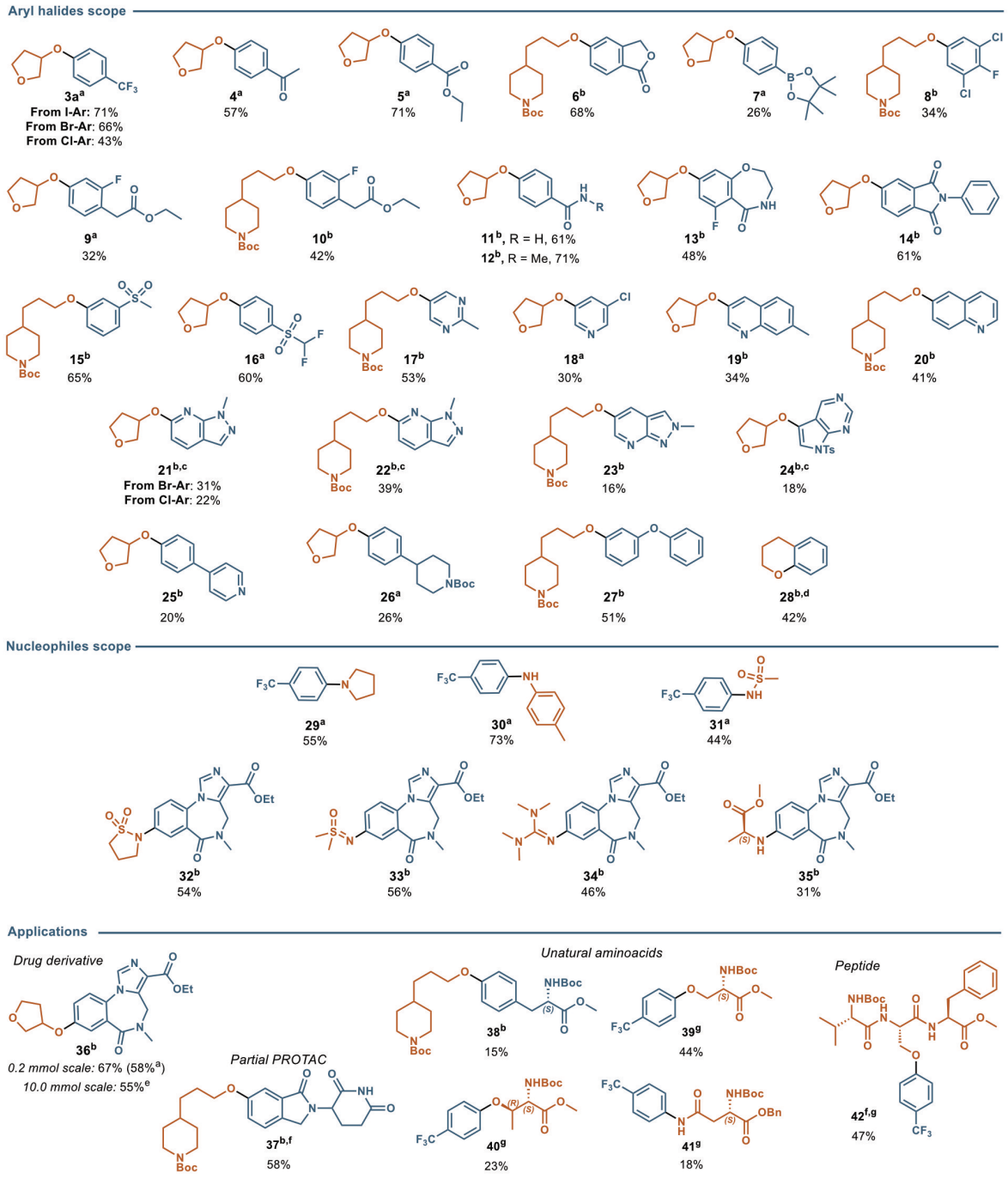

[a]Reaction conditions: Ar-Br (0.22 mmol, 1 equiv.), nucleophile (4 equiv.), quinuclidine (2.7 equiv.), $NiCl_2$.glyme (15 mol%), OMe_2bipy (18 mol%), DMF (2.2 mL, 0.1 M), 2x 1 mL sample loops, 0.2 mL chip mixer, 1 reactor (0.12 mm gap, 0.15 mL, 12 cm^2), 4.0 V, 1.5 Hz Square waveform, 0.05 mL/min, 3 min RT. [b]Reaction conditions: Ar-Br (0.22 mmol, 1 equiv.), nucleophile (4 equiv.), quinuclidine (2.7 equiv.), $NiCl_2$.glyme (15 mol%), OMe_2bipy (18 mol%), DMF (2.2 mL, 0.06 M), 2x 1 mL sample loops, 0.2 mL chip mixer, 2 reactors (0.12 mm gap, 2x0.15 mL, 2x12 cm^2, 0.15 mL tubing between 2 reactors), 4.0 V, 1.5 Hz Square waveform, 0.05 mL/min, 6 min RT. [c]More than 15% Ar-Ar byproducts were detected on the LC:MS of the crude mixture, see SI for details. [d]Intramolecular C-O coupling from 3-(2-bromophenyl)propan-1-ol (0.22 mmol). [e]Scale up performed with same equipment under exactly the same electrochemical conditions: Ar-Br (10 mmol, 1 equiv.), nucleophile (4 equiv.), quinuclidine (2.7 equiv.), $NiCl_2$.glyme (15 mol%), OMe_2bipy (18 mol%), DMF (90 mL, 0.11 M), 0.2 mL chip mixer, 2 reactors (0.12 mm gap, 2x0.15 mL, 2x12 cm^2, 0.15 mL tubing between 2 reactors), 4.0 V, 1.5 Hz Square waveform, 0.06 mL/min, 5 min RT. [f]Due to solubility issues, the concentration was decreased to 0.04 M. [g]Reaction conditions b were used with reverse stoichiometry: 1 equiv of nucleophilic aminoacid or peptide (0.22 mmol) and 4 equiv. of Ar-Br. In all cases, isolated yields are reported.

Figure 5. Aryl-halides scope, nucleophiles scope and application to PROTAC, amino acids and peptide.

organic base, room temperature, short retention time. Heterocycles including pyrimidine (**17**), pyridines (**18**), (iso)quinoline (**19**–**20**) and fused bicyclic structures (**21**–**24**) gave the corresponding targeted compounds could be isolated in practical synthetic yields. Notably, selectivity towards the desired ether products dropped in the presence of 2-bromopyridines (**21**–**22**) and a higher proportion of aryl-aryl coupling was detected (15–20 %, see Supporting Information for details). Electron-rich aromatic bromobenzenes bearing *para*-pyridine (**25**), alkyl (**26**), or ether (**27**) substituents gave moderate to good yields for the ether product despite the lower conversion of the starting aryl bromide. Chromane **28** can be prepared in 42 % isolated yield by intramolecular C–O arylation of 3-(2-bromophenyl)propan-1-ol.

The nucleophile scope could be extended beyond alkyl alcohols without modification of reaction conditions. A uniform set of conditions offers practical advantages for executing libraries, which often employ diverse building blocks to scan structure–activity relationships. Prior reports of electrochemical C–X arylation also highlight broad tolerance of nucleophile classes, but generally, reaction conditions are tailored by modification of the base, nucleophile equivalents[6c] or AC frequency.[6d] Under our DOE-optimized reaction conditions, C–N arylation proceeded efficiently with secondary alkyl amines (**29**) and electron-deficient amines, including anilines (**30**), sulfonamides (**31**–**32**), dimethylsulfoximine (**33**) and tetramethylguanidine (**34**).

Some limitations in substrate scope are listed in Figure S14. Nucleophile limitations include primary, linear amines that dimerize by amino-radical coupling (see SI), although branched primary amines, e.g., alanine methyl ester, was tolerated in moderate yield (31 % of **35**). Phenol completely inhibited the reaction, presumably by reversible oxidation under AC conditions. For a similar reason, using water as a nucleophile resulted in product inhibition, limiting the yield to 22 %. Coupling of tertiary alcohols such as *t*-butanol and 3-methyl-3-hydroxy *N*-Boc azetidine was challenging, returning unreacted starting material. Amongst the aryl halides screened, 5-membered heterocycles such as pyrazoles and imidazoles were unsuccessful, as were *ortho* substituted phenyl rings, consistent with prior results in batch.[6c] Importantly, aryl halide scaffolds containing alkyne or cyano groups were found to passivate the electrodes and inhibited subsequent reactions in the sequence.

Pleasingly, etherification of bromo-flumazenil **43**[23] generated the drug derivative **36** in 67 % isolated yield. This methodology could be applied to synthesize a new cereblon binder **37**, a molecule of interest for PROTAC applications. In addition, four unnatural amino acids were prepared by derivatization of protected bromo-phenylalanine (**38**), serine (**39**), threonine (**40**) and asparagine (**41**). More strikingly, arylation of the serine residue within a Boc-Val-Ser-Phe-OMe tripeptide **42** was demonstrated in 47 % isolated yield. To the best of our knowledge, this is the first example of electrochemical serine arylation of an oligopeptide. The synthesis of a drug derivative **36** could be scaled up to 10 mmol affording 2.06 g (55 % yield) in only 24 h without any further optimization nor changes in the electrochemical system (same voltage, frequency, interelectrode gap, no supporting electrolyte, see Supporting Information Figure S12), demonstrating the high flexibility of the platform.

To determine the utility of our system for parallel medicinal chemistry, two automated library sequences were performed with bromo-flumazenil **43** (Figure 6). We selected 30 alcohols and 30 amines with diverse functional groups and physiochemical properties. Reactions were performed under alternating voltage (4.0 V, 8 V_{pp}. 1.5 Hz SqWF), on a 150 µmol scale and 5 equivalents of nucleophile. Two electrochemical reactors were connected in series to enhance reaction conversions (see Supporting Information Figure S**11**). The total reaction time per run was ~45 minutes. Steady state current was typically recorded as ~30 mA, corresponding to ~4.7*F*/mol. Following sequence completion, reactions were analyzed by LCMS, and crude mixtures were submitted for high-throughput purification (HTP, see Supporting Information for details). The synthesis success rate was high for the C–O arylation library, with 24 out of 30 alcohols yielding satisfactory results (>20 % isolated yield). A variety of heterocycles and functional groups were successfully tolerated, such as ester (**46**), oxetane (**51**), diols (**52**,**60**), 1,2-*N*-Boc amino-alcohols (**54**), sulfone (**61**), pyridine (**71**), imidazole (**69**). Benzylic alcohol (**70**), a water surrogate showed good reactivity. Tertiary alcohols (**66**), phenol (**67**,**68**) and alcohol building blocks containing a tertiary amine (**49**), α-carbonyl (**50**), or an alpha-heteroatom (**56**) were unsuccessful.

The success rate of the C–N library was 20/30 (66 %). The selected moieties represented a diverse range of substituents, amine pKa and logP. Notable successful building blocks included cyclic (**73**–**76**, **78**–**80**) or acyclic (**82**–**84**) secondary amines, lactams (**97**–**98**), anilines (**92**–**93**,**95**), tertiary alkyl amines (**90**). Addition of ammonia could be achieved indirectly using *tert*-butyl carbamate (**101**) or benzophenone imine (**102**). Benzyl amine (**91**), indole (**96**) and hindered diisopropylamine (**81**) were not tolerated and primary amines (**86**–**89**) gave lower yields due to product dimerization under the electrochemical conditions (see Supporting Information for details and structures).

Conclusion

To conclude, we have developed a reproducible and broadly applicable method to enable electrochemical C–X (X=OH, NH) arylation in flow to access compound libraries. The flow cell gave significantly improved yields and selectivity compared to a batch parallel reactor. The application of potentiostatic alternating polarity across the flow cell was essential for consistency in sequential libraries and across scales (up to 10 mmol reported): the alternating polarity eliminated electrode passivation, improved reaction selectivity, enabled reactions to be performed in air, and removed the requirement for supporting electrolytes, which can complicate high throughput purification. This leap allows both sequential libraries and fast and consistent screening conditions. A DoE study identified optimal reaction con-

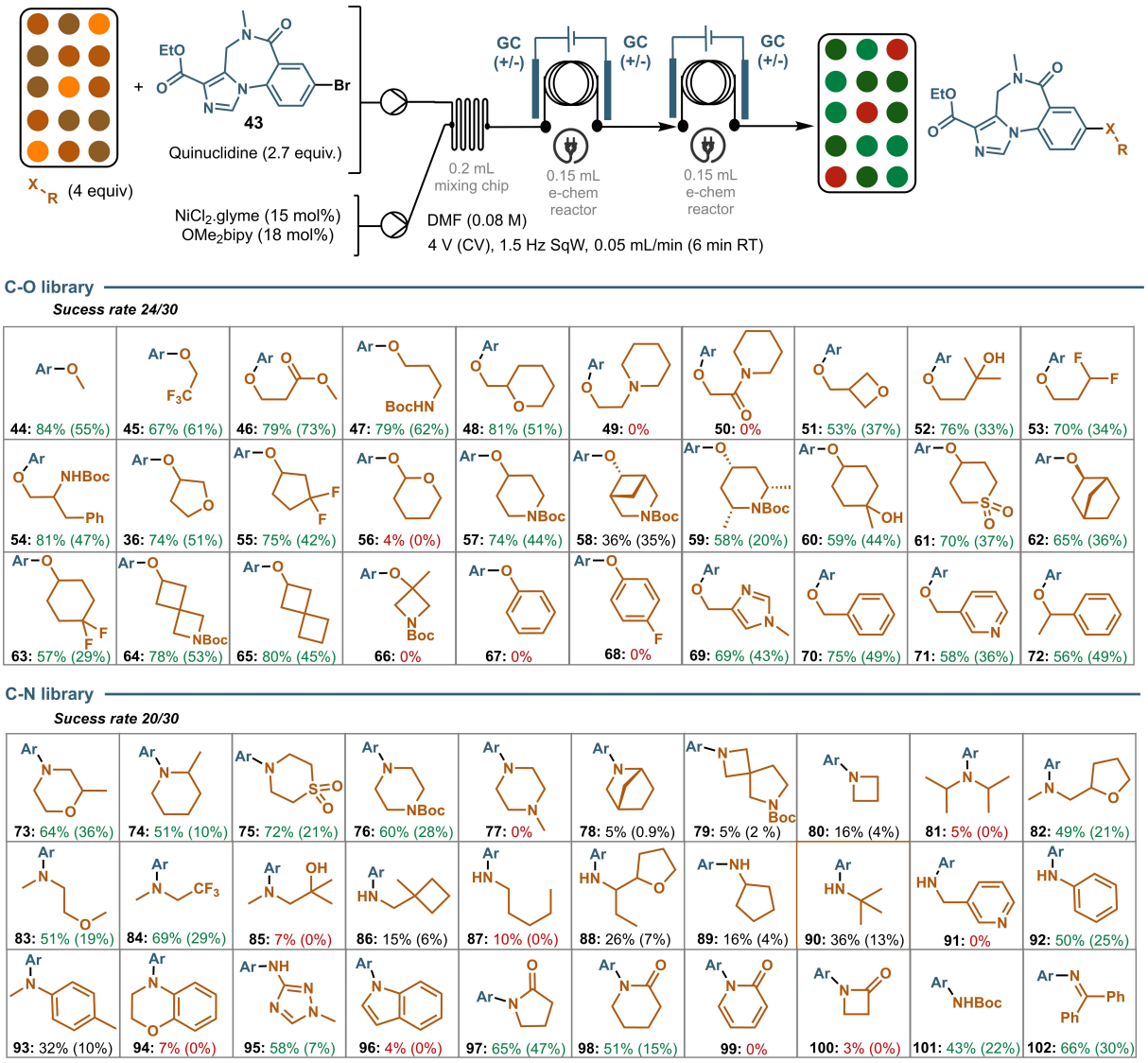

Figure 6. Automated library application—CO and CN functionalization of bromo-Flumazenil (LCMS integration reported (HTP yields in brackets)).

ditions and important non-linear interactions between chemical and electrochemical parameters. Consequently, one uniform reaction condition was applied to synthesize over 100 diverse C–O and C–N arylation products in an automated manner without the need for ligand or base variation. Of note for medicinal chemistry are the late-stage arylation of a serine-containing peptide and the wide application across heterocyclic scaffolds. Future directions include the application of flow AC to other paired-electrolysis reactions. Finally, the standardization of electrochemical equipment by academia and commercial suppliers plays a major role in the increasing adoption of electrochemistry in industry. Further improvements in cell design are always desirable to increase reactor productivity and control of electrochemical parameters.

Supporting Information

Experimental details, characterization data of compounds are provided. The authors have cited additional references within the Supporting Information.[5c,6a,24–26]

Acknowledgements

J.M. would like to thank V.I.E (Business France) for post-doctoral funding. B.T. thanks the European Union H2021 research and innovation program under the Marie S. Curie Grant Agreement (MiEL, No.101073003). We thank Bo Li and Soufyan Jerhaoui for peptide synthesis; Iris Maes, Kristien Raeymaekers, Alberto Fontana and Jose das Dores Sousa for purification and HRMS data; and Pavel Ryabchuk, Scott Wolkenberg, Zhicai Shi and Robin Kunkel (Fraunhofer ICT) for meaningful discussions.

Conflict of Interest

The authors declare no conflict of interest.

Data Availability Statement

The data that support the findings of this study are available in the supplementary material of this article.

Keywords: electrochemistry · compound libraries · nickel · flow chemistry · alternating polarity

[1] a) W. Liu, J. Mulhearn, B. Hao, S. Cañellas, S. Last, J. E. Gómez, A. Jones, A. De Vera, K. Kumar, R. Rodríguez, L. Van Eynde, I. I. Strambeanu, S. E. Wolkenberg, *ACS Med. Chem. Lett.* **2023**, *14*, 853–859; b) Z. Zhang, T. Cernak, *Angew. Chem. Int. Ed.* **2021**, *60*, 27293–27298.

[2] a) T. W. J. Cooper, I. B. Campbell, S. J. F. Macdonald, *Angew. Chem. Int. Ed.* **2010**, *49*, 8082–8091; b) N. H. Angello, V. Rathore, W. Beker, A. Wołos, E. R. Jira, R. Roszak, T. C. Wu, C. M. Schroeder, A. Aspuru-Guzik, B. A. Grzybowski, M. D. Burke, *Science* **2022**, *378*, 399–405.

[3] M. M. Heravi, Z. Kheilkordi, V. Zadsirjan, M. Heydari, M. Malmir, *J. Organomet. Chem.* **2018**, *861*, 17–104.

[4] G. Yashwantrao, S. Saha, *Tetrahedron* **2021**, *97*, 132406.

[5] a) Z. Chen, Y. Jiang, L. Zhang, Y. Guo, D. Ma, *J. Am. Chem. Soc.* **2019**, *141*, 3541–3549; b) K. Keerthi Krishnan, S. M. Ujwaldev, K. S. Sindhu, G. Anilkumar, *Tetrahedron* **2016**, *72*, 7393–7407; c) M. J. Strauss, M. E. Greaves, S.-T. Kim, C. N. Teijaro, M. A. Schmidt, P. M. Scola, S. L. Buchwald, *Angew. Chem. Int. Ed.* **2024**, *63*, e202400333.

[6] a) C. Li, Y. Kawamata, H. Nakamura, J. C. Vantourout, Z. Liu, Q. Hou, D. Bao, J. T. Starr, J. Chen, M. Yan, P. S. Baran, *Angew. Chem. Int. Ed.* **2017**, *56*, 13088–13093; b) H.-J. Zhang, L. Chen, M. S. Oderinde, J. T. Edwards, Y. Kawamata, P. S. Baran, *Angew. Chem. Int. Ed.* **2021**, *60*, 20700–20705; c) Y. Kawamata, J. C. Vantourout, D. P. Hickey, P. Bai, L. Chen, Q. Hou, W. Qiao, K. Barman, M. A. Edwards, A. F. Garrido-Castro, J. N. deGruyter, H. Nakamura, K. Knouse, C. Qin, K. J. Clay, D. Bao, C. Li, J. T. Starr, C. Garcia-Irizarry, N. Sach, H. S. White, M. Neurock, S. D. Minteer, P. S. Baran, *J. Am. Chem. Soc.* **2019**, *141*, 6392–6402; d) E. O. Bortnikov, S. N. Semenov, *J. Org. Chem.* **2021**, *86*, 782–793; e) C. Zhu, A. P. Kale, H. Yue, M. Rueping, *JACS Au* **2021**, *1*, 1057–1065; f) M. Boudjelel, J. Zhong, L. Ballerini, I. Vanswearingen, R. Al-Dhufari, C. A. Malapit, *Angew. Chem. Int. Ed.* **2024**, *63*, e202406203; g) For a review see, S. R. Waldvogel, S. Lips, M. Selt, B. Riehl, C. J. Kampf, *Chem. Rev.* **2018**, *118*, 6703–6755.

[7] a) I. Ghosh, N. Shlapakov, T. A. Karl, J. Düker, M. Nikitin, J. V. Burykina, V. P. Ananikov, B. König, *Nature* **2023**, *619*, 87–93; b) E. B. Corcoran, M. T. Pirnot, S. Lin, S. D. Dreher, D. A. DiRocco, I. W. Davies, S. L. Buchwald, D. W. C. MacMillan, *Science* **2016**, *353*, 279–283.

[8] N. E. S. Tay, D. Lehnherr, T. Rovis, *Chem. Rev.* **2022**, *122*, 2487–2649.

[9] G. Schneider, *Nat. Rev. Drug Discovery* **2018**, *17*, 97–113.

[10] B. Pijper, L. M. Saavedra, M. Lanzi, M. Alonso, A. Fontana, M. Serrano, J. Gomez, A. Kleij, J. Alcazar, S. Canellas, *JACS Au* **2024**, *4*, 2585–2595.

[11] a) A. S. Mackay, R. J. Payne, L. R. Malins, *J. Am. Chem. Soc.* **2022**, *144*, 23–41; b) Y. Kawamata, K. Hayashi, E. Carlson, S. Shaji, D. Waldmann, B. J. Simmons, J. T. Edwards, C. W. Zapf, M. Saito, P. S. Baran, *J. Am. Chem. Soc.* **2021**, *143*, 16580–16588.

[12] G.-Q. Sun, P. Yu, W. Zhang, W. Zhang, Y. Wang, L.-L. Liao, Z. Zhang, L. Li, Z. Lu, D.-G. Yu, S. Lin, *Nature* **2023**, *615*, 67–72.

[13] a) C. Kingston, M. D. Palkowitz, Y. Takahira, J. C. Vantourout, B. K. Peters, Y. Kawamata, P. S. Baran, *Acc. Chem. Res.* **2020**, *53*, 72–83; b) S. Maljuric, W. Jud, C. O. Kappe, D. Cantillo, *J. Flow Chem.* **2020**, *10*, 181–190; c) K. Lam, K. M. P. Wheelhouse, *Org. Process Res. Dev.* **2021**, *25*, 2579–2580.

[14] a) J. Rein, S. Lin, D. Kalyani, D. Lehnherr, in *The Power of High-Throughput Experimentation: General Topics and Enabling Technologies for Synthesis and Catalysis (Volume 1)*, (Eds.: M. Emmert, M. Jouffroy, D. C. Leitch) American Chemical Society, **2022**, pp. 167–187; b) J. Rein, J. R. Annand, M. K. Wismer, J. Fu, J. C. Siu, A. Klapars, N. A. Strotman, D. Kalyani, D. Lehnherr, S. Lin, *ACS Cent. Sci.* **2021**, *7*, 1347–1355.

[15] J. Fu, W. Lundy, R. Chowdhury, J. C. Twitty, L. P. Dinh, J. Sampson, Y.-H. Lam, C. S. Sevov, M. P. Watson, D. Kalyani, *ACS Catal.* **2023**, *13*, 9336–9345.

[16] a) D. Pletcher, R. A. Green, R. C. D. Brown, *Chem. Rev.* **2018**, *118*, 4573–4591; b) T. Noël, Y. Cao, G. Laudadio, *Acc. Chem. Res.* **2019**, *52*, 2858–2869; c) N. Petrović, B. K. Malviya, C. O. Kappe, D. Cantillo, *Org. Process Res. Dev.* **2023**, *27*, 2072–2081.

[17] J. Kuleshova, J. T. Hill-Cousins, P. R. Birkin, R. C. D. Brown, D. Pletcher, T. J. Underwood, *Electrochim. Acta* **2012**, *69*, 197–202.

[18] E. Rial-Rodriguez, J. D. Williams, D. Cantillo, T. Fuchß, A. Sommer, H.-M. Eggenweiler, C. O. Kappe, G. Laudadio, *ChemRxiv.* **2024**. DOI: 10.26434/chemrxiv-2024-dm4zj-v2.

[19] For recent reviews about AC, see: a) M. Jamshidi, C. Fastie, G. Hilt, *Synthesis* **2022**, *54*, 4661–4672; b) E. O. Bortnikov, S. N. Semenov, *Curr. Opin. Electrochem.* **2022** *35*, 101050; c) L. Zeng, J. Wang, D. Wang, H. Li, A. Lei, *Angew. Chem. Int. Ed.* **2023**, *62*, e202309620; d) A. P. Atkins, A. J. J. Lennox, *Curr. Opin. Electrochem.* **2024**, 101441. For report about electrode passivation under DC *vs* AC, see: e) A. F. Garrido-Castro, Y. Hioki, Y. Kusumoto, K. Hayashi, J. Griffin, K. C. Harper, Y. Kawamata, P. S. Baran, *Angew. Chem. Int. Ed.* **2023**, *62*, e202309157.

[20] N. Amri, R. A. Skilton, D. Guthrie, T. Wirth, *Synlett* **2019**, *30*, 1183–1186.

[21] Y. Mo, Z. Lu, G. Rughoobur, P. Patil, N. Gershenfeld, A. I. Akinwande, S. L. Buchwald, K. F. Jensen, *Science* **2020**, *368*, 1352–1357.

[22] C. Schotten, C. J. Taylor, R. A. Bourne, T. W. Chamberlain, B. N. Nguyen, N. Kapur, C. E. Willans, *React. Chem. Eng.* **2021**, *6*, 147–151.

[23] P. S. Kutchukian, J. F. Dropinski, K. D. Dykstra, B. Li, D. A. DiRocco, E. C. Streckfuss, L.-C. Campeau, T. Cernak, P. Vachal, I. W. Davies, S. W. Krska, S. D. Dreher, *Chem. Sci.* **2016**, *7*, 2604–2613.

[24] J. Sheng, X. Cheng, *CCS Chemistry* **2024**, *6*, 230–240.

[25] T. N. Ansari, R. H. Choudhary, M. Nachtegaal, A. H. Clark, S. V. Plummer, J. B. Jasinki, F. Gallou, S. Handa, *ACS Catal.* **2024**, *14*, 4099–4107.

[26] D. Meyer, H. Jangra, F. Walther, H. Zipse, P. Renaud, *Nat. Commun.* **2018**, *9*, 4888.

Manuscript received: July 16, 2024
Accepted manuscript online: October 9, 2024
Version of record online: November 7, 2024